Digital holographic interferometer using simultaneously three lasers and a single monochrome sensor for 3D displacement measurements

Tonatiuh Saucedo-A. [1,*], M. H. De la Torre-Ibarra[2], F. Mendoza Santoyo[2], Ivan Moreno[1]

[1]*Universidad Autónoma de Zacatecas, Calzada Solidaridad Esquina con Paseo la Bufa S/N, Zacatecas, C.P. 98060, México*

[2]*Centro de Investigaciones en Óptica, Asociación Civil, Loma Del Bosque 115, León Guanajuato C.P. 37150, México*

**tsaucedo@fisica.uaz.edu.mx*

Abstract: The use of digital holographic interferometry for 3D measurements using simultaneously three illumination directions was demonstrated by Saucedo et al. (Optics Express 14(4) 2006). The technique records two consecutive images where each one contains three holograms in it, e.g., one before the deformation and one after the deformation. A short coherence length laser must be used to obtain the simultaneous 3D information from the same laser source. In this manuscript we present an extension of this technique now illuminating simultaneously with three different lasers at 458, 532 and 633 nm, and using only one high resolution monochrome CMOS sensor. This new configuration gives the opportunity to use long coherence length lasers allowing the measurement of large object areas. A series of digital holographic interferograms are recorded and the information corresponding to each laser is isolated in the Fourier spectral domain where the corresponding phase difference is calculated. Experimental results render the orthogonal displacement components *u, v* and *w* during a simple load deformation.

OCIS codes: (090.2880) Holographic interferometry; (120.4290) Nondestructive testing; (120.5050) Phase measurement; (120.3940) Metrology.

References

1. C. M. Vest, *Holography Interferometry*, (Wyle, New York, 1979).
2. K. J. Gåsvik, *Optical Metrology*, (John Wiley & Sons Ltd., Chichester, 2002).
3. T T. Saucedo Anaya, M. De la Torre, and F. Mendoza Santoyo, "Microstrain detection using simultaneous endoscopic pulsed digital holography," Opt. Eng. **47**(7), 073601 (2008).
4. S. Schedin, G. Pedrini, H. J. Tiziani, and F. M. Santoyo, "Simultaneous three-dimensional dynamic deformation measurements with pulsed digital holography," Appl. Opt. **38**(34), 7056–7062 (1999).
5. M. De la Torre-Ibarra, F. Mendoza-Santoyo, C. Pérez-López, and S. A. Tonatiuh, "Detection of surface strain by three-dimensional digital holography," Appl. Opt. **44**(1), 27–31 (2005).
6. Z. Wang, T. Walz, H. R. Schubach, and A. Ettemeyer, "Three dimensional pulsed ESPI:technique of analysis of dynamic problems," Proc. SPIE **3824**, 58 (1999).
7. T. Saucedo A, F. M. Santoyo, M. De la Torre Ibarra, G. Pedrini, and W. Osten, "Simultaneous two-dimensional endoscopic pulsed digital holography for evaluation of dynamic displacements," Appl. Opt. **45**(19), 4534–4539 (2006).
8. A. T. Saucedo, F. Mendoza Santoyo, M. De la Torre-Ibarra, G. Pedrini, and W. Osten, "Endoscopic pulsed digital holography for 3D measurements," Opt. Express **14**(4), 1468–1475 (2006).
9. C. J. Mann, P. R. Bingham, V. C. Paquit, and K. W. Tobin, "Quantitative phase imaging by three-wavelength digital holography," Opt. Express **16**(13), 9753–9764 (2008).
10. Y. Fu, G. Pedrini, B. M. Hennelly, R. M. Groves, and W. Osten, "Dual-wavelength image-plane digital holography for dynamic measurement," Opt. Lasers Eng. **47**(5), 552–557 (2009).
11. I. Yamaguchi, T. Matsumura, and J. Kato, "Phase-shifting color digital holography," Opt. Lett. **27**(13), 1108–1110 (2002).

#128029 - $15.00 USD Received 11 May 2010; revised 6 Aug 2010; accepted 12 Aug 2010; published 3 Sep 2010

12. P. Picart, D. Mounier, and J. M. Desse, "High-resolution digital two-color holographic metrology," Opt. Lett. **33**(3), 276–278 (2008).
13. J.-M. Desse, P. Picart, and P. Tankam, "Digital three-color holographic interferometry for flow analysis," Opt. Express **16**(8), 5471–5480 (2008).
14. M. S. Millán, E. Valencia, and M. Corbalán, "3CCD camera's capability for measuring color differences: experiment in the nearly neutral region," Appl. Opt. **43**(36), 6523–6535 (2004).
15. C. van Trigt, "Visual system-response functions and estimating reflectance," J. Opt. Soc. Am. A **14**(4), 741–755 (1997).
16. A. Alsam, and R. Lenz, "Calibrating color cameras using metameric blacks," J. Opt. Soc. Am. A **24**(1), 11–17 (2007).
17. M. Takeda, H. Ina, and S. Kobayashi, "Fourier-transform method of fringe pattern analysis for computer based topography and interferometry," J. Opt. Soc. Am. **72**(1), 156–160 (1982).
18. T. Kreis, *Hand book of holographic Interferometry*, (Wiley-VCH, 2005).

1. Introduction

Digital holographic interferometry (DHI) is a full field, remote, non destructive and non invasive optical technique. It is based on the principle of holographic interferometry which has very high sensitivity for displacement measurements (a fraction of the wavelength used to illuminate the object ~λ/30) [1,2]. The surface displacement obtained can be associated with internal changes of the sample due to an external stimulus. The technique could be used in a wide variety of applications like a helpful tool to get detailed mechanical parameters from the sample under study such as micro strains [3]. Recent advances in electronics, lasers, and interferogram data analysis have facilitated the application of DHI in harsh environments away from controlled laboratory conditions. When performing experimental studies it is often necessary to have a 3D analysis of the sample's deformation to obtain the full description of its behavior along the commonly used orthogonal components *u, v* and *w*. At least three no-coplanar sensitivity vectors [4] are needed to calculate these components. One option is to have three illumination directions recording the interferograms sequentially [5]. However, in this case the drawback is the impossibility to use it when the deformation to be studied is not repeatable. Another option to this is to use three observation directions with three cameras [6]. However, the images have different object perspectives among them and a compensation algorithm has to be applied in order to reliably recover the information. Other proposed systems achieved simultaneous information illuminating from two or three directions, and using two or three lasers [7–10]. In these systems each object beam is matched with its corresponding reference beam with regards to their optical path lengths. In this way each hologram is recorded independently onto the CCD sensor. But this limits the system to observe small sample areas due the short coherence length required to meet the optical path matching. In what follows a system without the above restriction is described. It uses different lasers in order to have longer coherence lengths to allow the inspection of larger object areas. In the optical set up the lasers can be used with different wavelengths (e.g. three colors), a feature that will certainly assure an incoherent overlapping of the reference object beam pairs on the camera sensor, and still keep the desired large inspection area. Thus, each laser signal (reference-object beam pair) can independently be identified on the monochrome sensor. For simplicity, a three color configuration is used to ease the spectral observation of each laser due to the spatial frequency applied.

The later is a remarkable difference with systems recently proposed where two or three lasers with different wavelengths are used in the experiments. In these systems each wavelength is used as a codified channel which can be independently recovered by means of a color sensor [11,12]. These kind of systems may use: mosaic, 3CCD or stack color sensors. These are limited to the spectral response of each color in the sensor according to its configuration [13–16]. For this reason each wavelength is well established in order to avoid any overlapping among them.

In our experiment, a monochrome sensor with a high quantum efficiency response is used, and each reference-object beam pair interference signal is resolved in the Fourier domain in

#128029 - $15.00 USD Received 11 May 2010; revised 6 Aug 2010; accepted 12 Aug 2010; published 3 Sep 2010

order to obtain three independent phase maps that are used to calculate the three orthogonal displacement components *u*, *v* and *w*. Experimentally and in order to prove our proposed method, a simple load test is performed using a smooth object surface.

2. Method

The system is based in the principle of the superposition of several holograms independently resolved in the spectral domain (see ref. 8), i.e., non coherent to each other. In this case, the intensity (*I*) registered by the sensor along the *x* and *y* directions can be expressed by:

$$I(x,y)=\sum_{m=1}^{3} I_{\lambda m}(x,y)=\sum_{m=1}^{3}\left[\left|R_{\lambda m}(x,y)+O_{\lambda m}(x,y)\right|^{2}\right], \tag{1}$$

where λ_m represents each of the three different laser wavelengths (m = 1, 2, 3). The couple $R_{\lambda m}$ and $O_{\lambda m}$ are the reference and object beam pair corresponding to each laser and illumination position. Once this first image is obtained, a second one (I') with a deformation applied to the object is recorded. Then each image is Fourier transformed to process each laser wavelength independently from the others [17,18], producing its corresponding wrapped phase map:

$$\Delta\varphi_{\lambda m}(x,y)=\varphi'_{\lambda m}(x,y)-\varphi_{\lambda m}(x,y), \tag{2}$$

where $\Delta\varphi_{\lambda m}$ is the relative phase-difference map for each wavelength (m = 1, 2, 3). $\varphi_{\lambda m}$ and $\varphi'_{\lambda m}$ are the phase maps for each wavelength before and after the deformation respectively. Once the three wrapped phase maps are obtained, it is necessary to unwrap them, for instance using the commercially available software (Pv_spua2 by Phase Vision Ltd.). With these unwrapped phase maps and considering the geometry of the optical set up, see Fig. 1, the displacement components (*u, v, w*) can be associated as follows,

$$\begin{bmatrix}\Delta\varphi_{\lambda_1}\\ \Delta\varphi_{\lambda_2}\\ \Delta\varphi_{\lambda_3}\end{bmatrix}=2\pi\begin{bmatrix}-\sin\theta/\lambda_1 & 0 & (\cos\theta+1)/\lambda_1\\ \sin\theta/\lambda_2 & 0 & (\cos\theta+1)/\lambda_2\\ 0 & -\sin\theta/\lambda_3 & (\cos\theta+1)/\lambda_3\end{bmatrix}\begin{bmatrix}u\\ v\\ w\end{bmatrix}, \tag{3}$$

from this expression, θ is the angle between the illumination and observation direction with the same value for each laser (see Fig. 1b). Using this equation it is possible to obtain the three orthogonal displacement components *u*, *v* and *w* independently using just two digital holographic interferograms.

3. Experimental procedure

Figure 1(a) shows the schematic view of the optical system where three different sources of illumination are used. The first one is an Argon-ion laser with λ_1 = 458 nm and 50mW output power, attenuated to 25 mW by means of a neutral density filter (NDF1). The second one is a diode pumped solid state cw Nd:YAG laser with λ_2 = 532 nm with maximum output power of 500mW, attenuated to 25 mW by NDF2. Finally, a He-Ne laser at λ_3 = 633 nm with 25mW output power. The intensity adjustment procedure is made in order to match a similar signal within the sensor's dynamic range, according with its quantum efficiency for each wavelength. Each laser beam is divided into an object and a reference beam using BS1, BS2 and BS3 respectively.

#128029 - $15.00 USD Received 11 May 2010; revised 6 Aug 2010; accepted 12 Aug 2010; published 3 Sep 2010

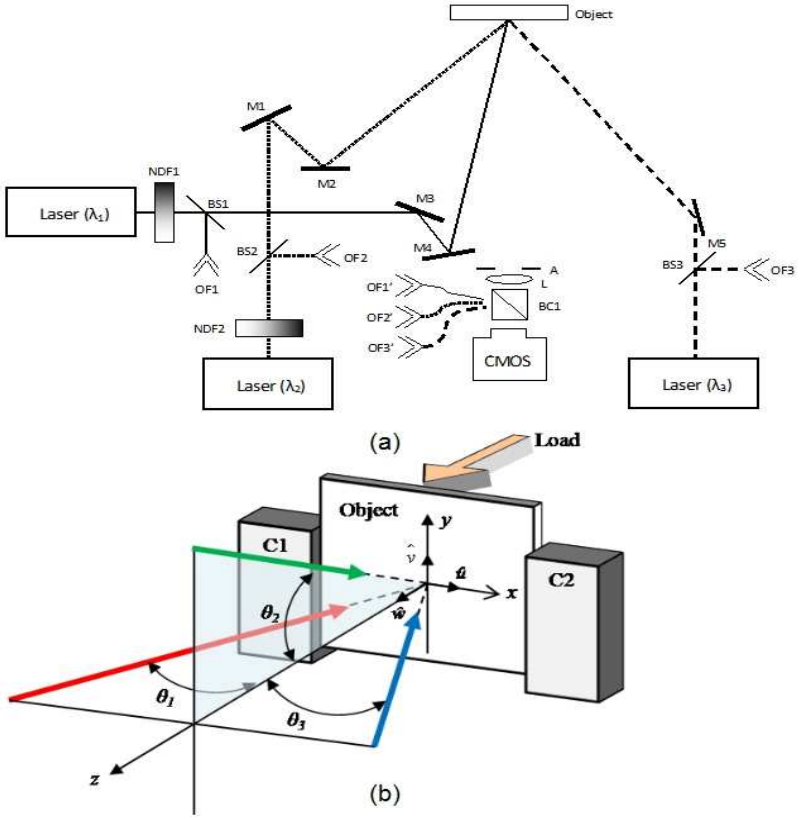

Fig. 1. Experimental setup (a) Schematic view of the optical set up using three lasers, (b) Mechanical rig used to illuminate and constrain the sample under study. From this geometry $\theta_1 = \theta_2 = \theta_3 = \theta$.

The object beam from λ_1 is directed onto the object using two mirrors (M3 and M4) and a 10X microscope objective to illuminate the object. The reference beam is launched into a single mode fiber (OF1) with the other terminal (OF1') attached near the beam combiner (BC1). A similar reference and object illumination procedure is followed for λ_2 and λ_3. All reference beam terminals (OF1', OF2' and OF3′) are placed at the same relative distance to BC1. The angles made by the unit vectors from each observation and illumination directions are the same, i.e., the angle θ is the same for all observation-illumination unit vector pairs. The maximum spatial frequency that can be recorded with the CMOS camera used is given by $f_{max} = D/z\lambda$, where D is the aperture diameter and z is the distance measured from the centre of the lens to the sensor arrangement. The smallest wavelength is used to calculate the aperture which in this case is 3.6mm.

#128029 - $15.00 USD Received 11 May 2010; revised 6 Aug 2010; accepted 12 Aug 2010; published 3 Sep 2010

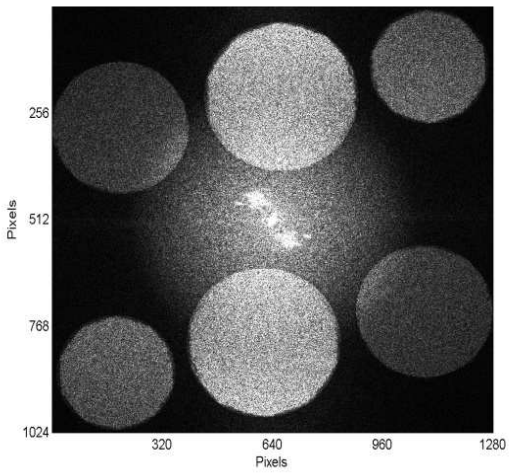

Fig. 2. Fourier spectrum showing the spectral distributions for each laser in a single hologram. The upper three circles from left to right are λ_2, λ_1 and λ_3 respectively. The lower three circles are the corresponding complex conjugate terms.

A spatial carrier frequency is introduced for each laser wavelength in order to resolve them independently in the Fourier space (see Fig. 2). The object under study is a plastic plate which is deformed applying a load behind it, i.e., producing a deformation. A mechanical press (C1 and C2 in Fig. 1b) is used to hold the plate to avoid any uncontrolled movement. Figure 1b shows in detail the illumination distribution and the load applied behind the sample. The press tightly holds the object in the *x* axis leaving the *y* and *z* axis free to move. The field of view (FOV) of the system is 25.6 X 20.5 mm using a lens (L) with 25 mm of focal length, which images the object onto the CMOS camera (Pixelink with 1280 X 1024 pixels). Two images are then recorded, one with the object without a load and a second one with the load applied. Once both image interference holograms are processed three wrapped phase maps are obtained. Figures 3a, 3b and 3c show the displacement observed with λ_1, λ_2 and λ_3 respectively.

As expected due to the geometry used in the optical set up, Fig. 3a contains more fringes due the shorter wavelength used, as opposed to Fig. 3c where the same load renders fewer fringes due to a larger wavelength. In all cases the illumination angle (θ) between the object beam and the observation unit vectors is 23°. Once these three phase maps are unwrapped they give the same displacement for each case.

#128029 - $15.00 USD Received 11 May 2010; revised 6 Aug 2010; accepted 12 Aug 2010; published 3 Sep 2010

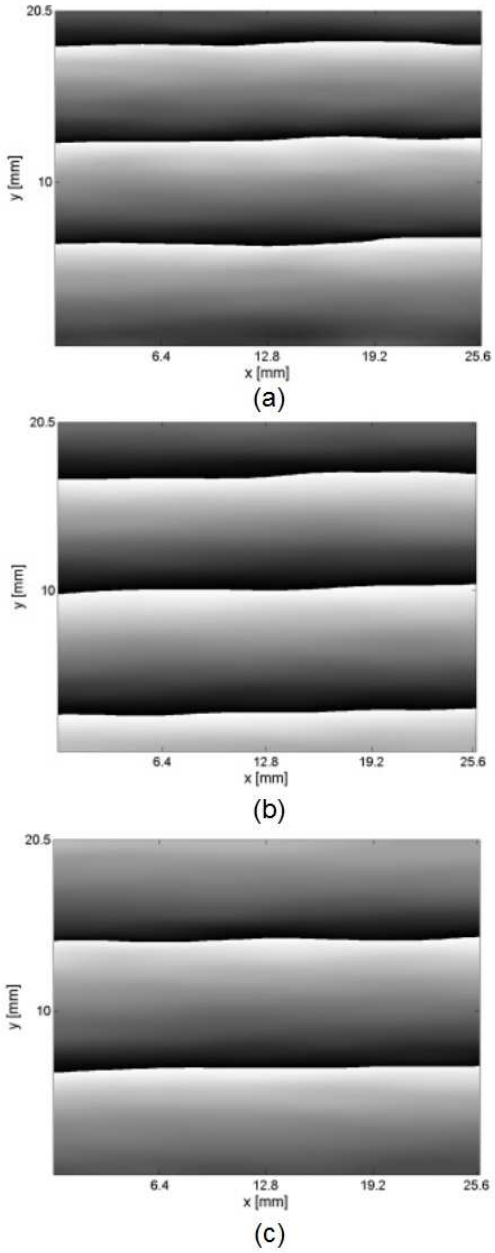

Fig. 3. Wrapped phase maps for (a) Argon-ion (λ_1 = 458 nm) (b) diode pumped CW Nd:YAG (λ_2 = 532 nm), and (c) He-Ne (λ_3 = 633 nm) lasers, showing deformation variations between -π and π (black and white respectively).

Using Eq. (3) it is possible to generate a mesh grid for each orthogonal displacement as Fig. 4a, 4b and 4c shows.

#128029 - $15.00 USD Received 11 May 2010; revised 6 Aug 2010; accepted 12 Aug 2010; published 3 Sep 2010

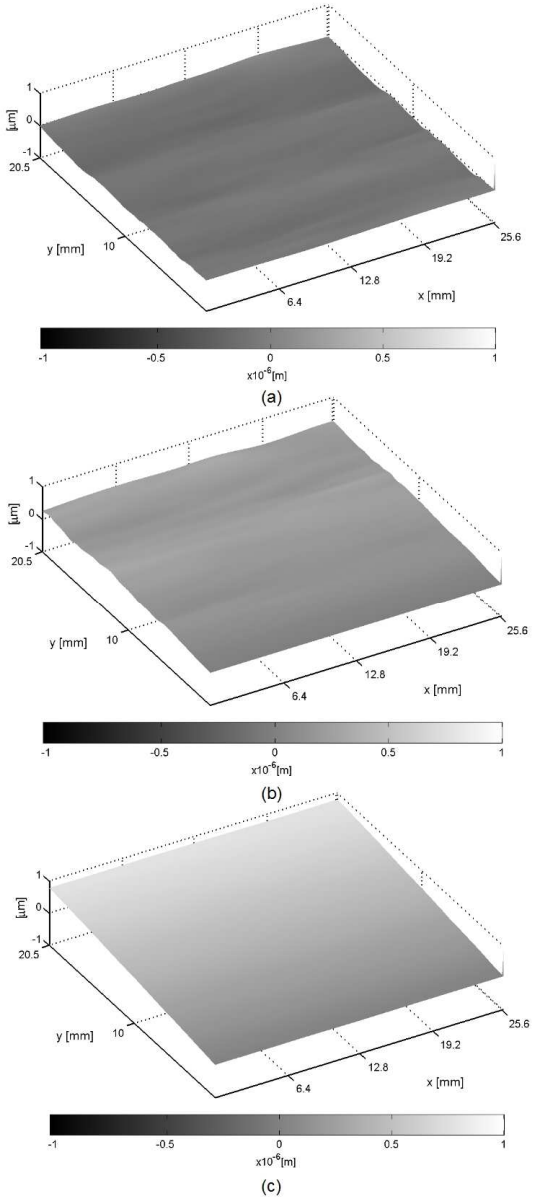

Fig. 4. Orthogonal displacement components (a) *u* (b) *v* and (c) *w* obtained with the wrapped phase maps shown in Figs. 3a, 3b and 3c respectively.

Figure 4a shows the *u* component whose magnitude is in a good agreement with the mechanical constrains applied to the sample during the load. The *w* displacement component shows an expected behavior due to the kind of deformation applied as Fig. 4c shows. A similar response is observed in Fig. 4b where the *v* component is shown. The x and y axes in Fig. 4 represents the FOV while the other one represents the displacement component for each case.

4. Discussion

In the present work we showed an optical system which measures displacements over large and smooth surfaces. However, height changes in rough surfaces will introduce errors in the

#128029 - $15.00 USD Received 11 May 2010; revised 6 Aug 2010; accepted 12 Aug 2010; published 3 Sep 2010

measurements. This is due to the angles of illumination and the technique *per se*, something already reported in reference 9. As Fig. 2 shows the use of three lasers can introduce an undesired overlapping of the central term with the rest. This overlapping can introduce noise if a filtering algorithm to avoid it is not used. This has been mentioned in reference 10 where a Fourier window algorithm was applied. In order to show the ability of our system to measure a more complex deformation a second test was performed. In this second test the same object is heated from behind its surface using an electric resistor with a tip. Figure 5 shows the three displacement components *u*, *v* and *w* where a melting is observed in the object's surface.

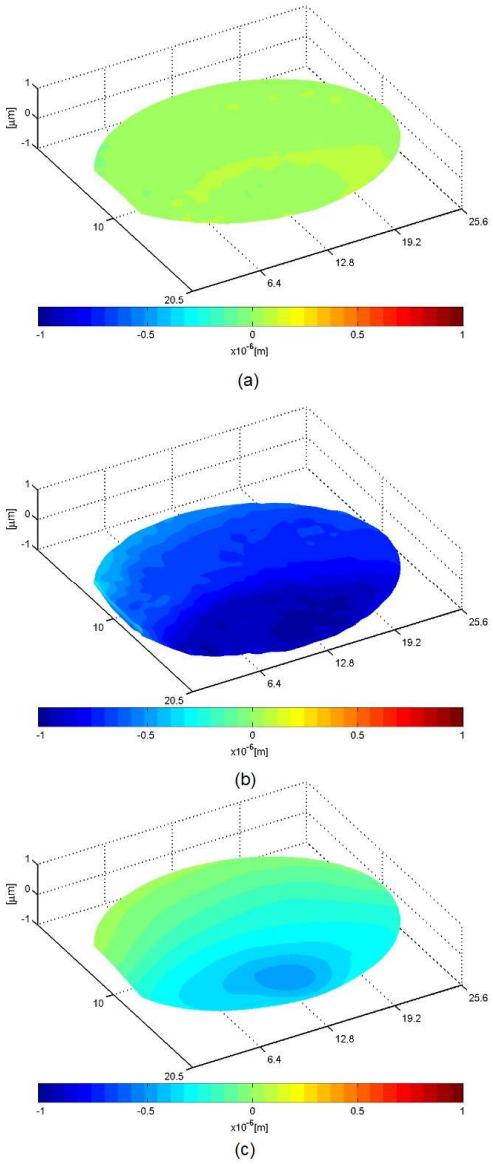

Fig. 5. Orthogonal displacement components (a) *u* (b) *v* and (c) *w* obtained during the heating test.

#128029 - $15.00 USD Received 11 May 2010; revised 6 Aug 2010; accepted 12 Aug 2010; published 3 Sep 2010

5. Conclusions

It is possible to obtain the orthogonal displacement components for a non repeatable event using DHI with the proposed optical system. Just one image is required to have embedded simultaneously three digital holographic interferograms. Two consecutive images are individually processed to obtain a 3D study of the sample. We are at present investigating the possibility to use the three different wavelength displacements to perform object contouring, a feature that will distinguish the present technique as one that would obtain the orthogonal displacements and sample surface shape with only two images. If one wishes to perform simultaneous data acquisition from three illumination directions using different lasers, the later avoids the need to use an optical source with short coherence for illumination. In the optical set up described above there is no restriction to use necessarily three different colors (RGB, etc) to obtain the 3D measurement. The later is possible because the system does not use a color sensor as codifier.

#128029 - $15.00 USD Received 11 May 2010; revised 6 Aug 2010; accepted 12 Aug 2010; published 3 Sep 2010